REPORT DOCUMENTATION PAGE

AFRL-SR-AR-TR-03-

0265

Form Approved OMB No. 0704-0188

1. AGENCY USE ONLY (Leave blank)	2. REPORT DATE	3. REPORT TYPE AND DATES COVERED
		15 Aug 2002- - 14 Feb 2003 Final Report

4. TITLE AND SUBTITLE	5. FUNDING NUMBERS
(SBIR) Dynamically Tunable Photonic Bandgap Crystal Components BMDO02-011	65502C 6016/01
6. AUTHOR(S) Dr Lawrence	
7. PERFORMING ORGANIZATION NAME(S) AND ADDRESS(ES) TESLA TECHNOLOGIES INC 9040 EXECUTIVE PARK DR SUITE 385 KNOXVILLE TN 37923	**8. PERFORMING ORGANIZATION REPORT NUMBER**
9. SPONSORING/MONITORING AGENCY NAME(S) AND ADDRESS(ES) AFOSR/NE 4015 WILSON BLVD SUITE 713 ARLINGTON VA 22203	**10. SPONSORING/MONITORING AGENCY REPORT NUMBER** F49620-02-C-0078

11. SUPPLEMENTARY NOTES

20030731 056

12a. DISTRIBUTION AVAILABILITY STATEMENT	12b. DISTRIBUTION CODE
APPROVED FOR PUBLIC RELEASE, DISTRIBUTION UNLIMITED	

13. ABSTRACT *(Maximum 200 words)*

Periodic photonic crystal structures channel electromagnetic waves much as semiconductors/quantum wells channel electrons. Photonic bandgap crystals (PBC) are fhbricated by arranging sub-wavelength alternating materials with high and low dielectric constants to produce a desired effective bandgap. Photons with energy within this bandgap cannot propagate through the structure. This property has made these structures usefthl for microwave applications such as frequency-selective surfaces, narrowband filters, and antenna substrates when the dimensions are on the order of millimeters. They are also potentially very useftil, albeit much more difficult to fabricate, in the visible/near-infrared region for various applications when the smallest dimensions are at the edge of current mierolithography fabrication tools. We micro-fabricated suspended ftee standing micro-structure bridge waveguides to serve as substrates for PBC features. These micro-bridges were fabricated onto commercial silicon-on-insulator (SOT) wafers. Nanoscale periodic features were fabricated onto these micro-structure bridges to form a tunable system. When this combined structure is perturbed, such as mechanical deflection of the suspended composite structure at resonance, there can be a realtime sbifl in the material effective bandgap due to slight geometric alterations due to the induced mechanical stress. Extremely high resonance frequencies/device speeds are possible with these very small dimension MEMS.

14. SUBJECT TERMS	15. NUMBER OF PAGES
	16. PRICE CODE

17. SECURITY CLASSIFICATION OF REPORT	18. SECURITY CLASSIFICATION OF THIS PAGE	19. SECURITY CLASSIFICATION OF ABSTRACT	20. LIMITATION OF ABSTRACT
UNCLASSIFIED	UNCLASSIFIED	UNCLASSIFIED	UL

SBIR Phase I
Final Report

Contract Number: **F49620-02-C-0078**

Project Title: **Dynamically Tunable Photonic Bandgap Crystal Components**

Contractor: **Tesla Technologies Inc.**
P.O. Box 31378
Knoxville TN 37930
Tel. 865-531-9150
E-mail: tti@TeslaTechInc.com

Report Number: **TTI08152002FR**

Dynamically Tunable Photonic Bandgap Crystal Components

W.R. Lawrence , P.G. Datskos and S. Rajic

Tesla Technologies Inc., P.O. Box 31378, Knoxville TN 37930
University Of Tennessee, Neilson Physics Building, Knoxville, TN 37996

Abstract

Periodic photonic crystal structures channel electromagnetic waves much as semiconductors/quantum wells channel electrons. Photonic bandgap crystals (PBC) are fabricated by arranging sub-wavelength alternating materials with high and low dielectric constants to produce a desired effective bandgap. Photons with energy within this bandgap cannot propagate through the structure. This property has made these structures useful for microwave applications such as frequency-selective surfaces, narrowband filters, and antenna substrates when the dimensions are on the order of millimeters. They are also potentially very useful, albeit much more difficult to fabricate, in the visible/near-infrared region for various applications when the smallest dimensions are at the edge of current microlithography fabrication tools. We micro-fabricated suspended free standing micro-structure bridge waveguides to serve as substrates for PBC features. These micro-bridges were fabricated onto commercial silicon-on-insulator (SOI) wafers. Nanoscale periodic features were fabricated onto these micro-structure bridges to form a tunable system. When this combined structure is perturbed, such as mechanical deflection of the suspended composite structure at resonance, there can be a realtime shift in the material effective bandgap due to slight geometric alterations due to the induced mechanical stress. Extremely high resonance frequencies/device speeds are possible with these very small dimension MEMS.

1. Introduction

Periodic photonic crystal structures channel electromagnetic waves much as semiconductors/quantum wells channel electrons. Photonic bandgap crystals (PBC) can be realized by arranging sub-wavelength alternating materials with high and low dielectric constants, as shown from our recent demonstration in Figure 1, to produce a desired effective bandgap. Photons with energy within this bandgap cannot propagate through the structure [1]. This property has made these structures useful for microwave applications such as frequency-selective surfaces, narrowband filters, and antenna substrates when the dimensions are on the order of millimeters. They are also potentially very useful, albeit much more difficult to fabricate, in the visible/infrared region for various applications when the dimensions of the substrate range from 40 nm to 1,500 nm. PBC research has grown tremendously over the last few years [2]. However, the few demonstrations to date have typically involved passive devices with no provision for bandgap tuning. The exceptions have been two PC tuning demonstrations in which either a swelling membrane or a thermally expanding surface were used to affect the periodicity [3,4]. These methods of optical property tuning are slow and primarily used for chemical detection instead of integrated photonic device applications.

2. Tunable PBC Concept

Nanoscale periodic structures fabricated onto micro-structure substrate waveguides can form a tunable system with two sets of mirrors (holes) separated by a microcavity (gap), as shown in Figure 2. When this combined structure is perturbed, such as mechanical deflection of the suspended composite structure at resonance, there can be a substantial and realtime shift in the material effective bandgap due to the periodicity alteration resulting from strain. Even more control of optical properties can be achieved if part of the released waveguide is placed in tension and part of it is placed in compression. These two sections of the suspended PBC waveguide can be made to resonate in phase, or any degree out of phase, to more fully control the optical properties of the PBC. The optical properties of photonic crystals are extremely sensitive to minor periodicity, index, and especially gap spacing changes. Theoretical work has been published indicating that a mere 3% shear strain can be used to tune 73 % of the original undistorted absolute bandgap [5]. Thus a much smaller stress could still produce an extremely useful device.

Several useful architectures and devices can be envisioned from spectrally tunable components based on the micro-bridge structure shown in Figure 2, including modulators, optical filters, optical switches, WDM, optical logic circuits, variable attenuators, power splitters, isolators, etc. Although not attempting spectral tuning, these types of physical structures were previously demonstrated at MIT and can serve as useful component substrates for our tunable PBC work since their properties are understood and accepted [6]. Figure 3 shows a node that is a very powerful building block of this approach. Multiple strain tunable PBC microbridges are shown interconnected. If the nominal optical path through the shaded PBC waveguide is across bridges A and B, then the unperturbed propagation condition will be satisfied by the choice of dielectric constant variations (waveguide holes) to allow a straight path to be permissible. By actuating suspended waveguide bridges A and B with electric fields, acoustics energy, out of band photons, etc., an efficient reflected resonance condition can be induced to inhibit propagation within a given wavelength region. Thus, an effective bandgap condition is established for certain wavelengths that extinguishes that direction as a viable path. Although the physics is different, the electronic bandgap of a crystal material would similarly inhibit propagation, but through absorption instead of reflection. Many such bridges can be fabricated serially to form a tunable filter with substantial dynamic range. However, if micro-bridge C were simultaneously actuated with the correct phase difference and amplitude to set-up a resonant condition such that propagation through path A and C were permitted for a given wavelength, additional capabilities would be established. In this case, path A-B would be strongly attenuated while path A-C would be simultaneously highly transmissive. The node between micro-brides A, B, and C could represent an optical switch, optical logic gate segment, or a small part of a WDM architecture. The different possible paths, A-B and A-C are selectable according to wavelength. Ultimately, large networks of such nodes can be envisioned for large scale integration.

3. Mechanical and Optical Modeling

Our mechanical modeling using ProEngineer software indicates that, for very short structures, resonant frequencies approaching 10 GHz are possible which will fit well with the device speed requirements for many envisioned and future applications. The response times, calculated at the resonant frequency, of various potential dielectric materials and geometries, indicate that operation of these tunable devices can be very high-speed for realistic implementations. We have calculated the moment of inertia for a simple beam rigidly supported at both ends and then solved for the resonant frequency for four different materials and six different beam (waveguide) lengths [7,8]. All of the calculated waveguide widths and thicknesses were fixed at 2000 and 500 nm, respectively. We can get a good initial idea of potential device speed from table I.

We next examined the amount of possible length perturbation for these devices. This length change is the mechanism that produces the optical property alterations. The nominal material chosen was silicon and the devices were modeled at resonance at an equivalent intensity that corresponded to half the material yield strength. An immediate limitation to this mechanical stress based spectral tuning approach can be seen when the single layer waveguide material is used. If a suspended micro-bridge waveguide were stressed to induce a downward curvature then the top of the structure would be in tension and the bottom would be in compression. The average period and gap lengths will not change in most cases. The simple solution to this impasse is the fabrication of the active waveguide material onto another, lower index material, which will still guide the photons but will also induce a shift in the neutral stress axis of the entire structure, thereby causing the entire active waveguide to be entirely in tension or compression during mechanical resonance motion. The real breakthrough came during mechanical modeling of these devices that showed that if the PBC alternating dielectric region (holes) of the micro-bridge were shifted to one side of center, then there will be times during mechanical resonant motion for certain modes of vibration that all of the active waveguide region can be either in tension or compression. Thus a de-centered region exists were the stress gradient is extremely flat for part of the mechanical oscillation cycle. This means that a single layer/material waveguide device can be designed which is much more efficient and easier to fabricate as shown in Figure 4. Table II shows the magnitude of length perturbation that is possible with this type of approach given the materials and geometries chosen for this mechanical model. OPTIWAVE software was used to model the expected spectral shift due to the given stress based mechanical perturbation predicted by the ProEngineer software. The finite difference time domain (FDTD) module of this software was used to produced a change from nominal wavelength in resonant optical transmission of 40.1 nm, 25.2 nm, and 15.3 nm for the three conditions shown in Table II. Figure 5 shows the wavelength shift for the above mention perturbation.

4. Micro/Nano Fabrication

Near IR (1300 & 1550 nm) PBC operation is just about at the limit of present state-of-the-art photolithography since the smallest feature sizes can be as small as one tenth of the operational wavelength. Therefore new schemes were required to proceed with this application and for future visible applications that require sub-100 nm features. We have been developing several fabrication techniques that were used in this research effort. All are direct write techniques due to the dimensions required and the fact that we were only attempting to demonstrate the feasibility of the approach during this first phase of the project.

The most promising of these nanofabrication approaches that we have been developing is Atomic Force Microscopy (AFM) nano-oxidation masking. This technique involves applying electric fields of a few volts between a conductive AFM tip and a conducting or semiconducting surface, such as titanium, in the presence of a controlled humidity environment. The presence of the oxygen atoms in the water vapor will cause an oxidation of the surface that is extremely localized since the field will drop-off exponentially away from the approximately 20 nm radius AFM tip. The oxidation depth is typically only a few nanometers, however, this is a sufficiently thick oxide mask to chemically etch nano-scale features. Control of the relative humidity of the AFM instrument is very crucial for this extremely precise nano-scale masking technique. The advantage of this approach is that it is photo-resist free and can produce very fine details on a properly prepared surface.

Electron beam lithography is a photo-resist based approach and was the most standard technique used in this feasibility demonstration since the initial and most useful operation wavelengths are in the near IR. The photoresist in this technique is exposed with a focused electron beam. Since the equivalent particle wavelength of an electron is very small, a direct focusing of the beam can be used to achieve a small exposure spot size with no need for subaperture masking. Spot sizes resulting in exposed photoresist areas of less than 20 nm diameter are possible with this direct write technique. However, the limiting feature size is often the polymerization of the exposed photoresist that is larger than the illuminated spot size. Since electrons are also charged particles, high beam currents can also result in a widening of the beam spot size.

Sub-aperture Near-Field Scanning Optical Microscopy lithography is another direct write technique that uses an extremely small opening in the end of a tapered optical fiber to expose photoresist. The fiber is typically tapered to a radius of several tens of nanometers. The small radius fiber end is then coated with a metal such as aluminum and an even smaller aperture is thus defined producing a substantially subwavelength optical opening. Since this technique uses conventional photoresist and the exposure wavelength is in the UV, the diameter of the optical opening is thus typically less than 40 nm. As in the case of the AFM lithography mentioned above, subnanometer vertical (z-axis) control is possible with a piezotube controlled x-y scanning capability that is used to define the desired pattern.

Another photo-resist free fabrication technique used was chemically enhanced focused ion beam direct write patterning. This technique uses a 30 KeV beam of focused gallium ions accelerated at a target point with diameters as small as 20 nm. Since these are also charged particles, if the beam current is large, the particles will begin to repel each other and the beam size may expand beyond 1000 nm. Since accelerated ions posses substantial kinetic energy, collisions with a surface result in material removal. On average, one gallium ion will remove one target atom from the work surface in one collision. This can produce very detailed nano-scaled features by directly milling a pattern into a target surface. However, if a chemical etchant/binder is introduced near the surface in the path of the ion beam, a chemically enhanced, increased material removal will result. Accelerated material removal of a factor of 20 times can be achieved.

Silicon-on-insulator (SOI) starting substrate material was primarily used, however, for operation below 1.1μm simple deposited oxide was also possible. With the single crystal silicon acting as the waveguide material, operation at the important telecommunications wavelengths of 1300 and 1550 nm was achievable. The nominal wafer cross section consisted of a 0.5 mm silicon substrate containing 380 nm of SiO_2 that is capped with a 280 nm single crystal silicon layer (waveguide). The wafers were patterned with multiple techniques described above and then etched with HF acid to undercut the glass and release the suspended bridge. Figure 6 shows the fabricated devices on SOI substrates. These particular dimension work could have been performed with state-of-the-art photolithography equipment, however, MEMS fabrication is typically at least two generations behind integrated circuit fabrication facilities due to availability. Therefore, if operation in the visible is eventually required (photonic crystal feature sizes of 40 - 70 nm) then an alternate fabrication method must be employed for the near future.

5. Conclusions

Our mechanical modeling showed that a PBC waveguide can be used to produce preferentially compressive and tensile forces within a suspended micro-bridge. These mechanical perturbations in the hole spacing and micro-cavity gap were substantial in even single layer structures. That information was fed into our optical modeling which indicates the feasibility of stress based spectral tuning sufficient for many practical applications.

All of the fabrication techniques used in this work were direct write due to the small feature sizes required and because most MEMS fabrication facilities employ several generations old photolithographic tools. Although AFM nano-oxidation is essentially another direct write technique, recent demonstrations of AFM operation with two dimensional cantilever arrays (32x32) could potentially write approximately 1000 features simultaneously. Further advances to an envisioned 1000x1000 array would produce substantial parallel fabrication capabilities with this approach, while still producing less than 50 nm feature sizes. This would then make scale-up of visible wavelength PBC based devices feasible. Table three summarizes the micro/nano-fabrication study including an attempt with single point diamond turning. The vertical direction can essentially be on the angstrom scale under ideal conditions for the chemical material removal processes on polished substrates. A limitation on the photoresist based processes (NSOM, EBL) is often the unintended polymerization beyond the exposed area. The charged particle based processes (FIB, EBL) require low beam currents due to the repulsion and beam spreading of similarly charged particles when focusing at the nano scale. The AFM approach has the precision and, unfortunately, the speed of AFM instruments unless parallel readout micro-cantilevers are employed.

A rigorous testing regime is needed to experimentally verify the premise of this work. An additional implementation approach we will investigate more fully in the future is the combination of photonic bandgap tunable architecture in a GaAs/GaAlAs multiple quantum well epitaxial film to enhance the spectral tuning. This work would involve the strain induced manipulation of both electronic and photonic (effective) bandgaps. We have previously examined the use of pressure/strain dependance of the bandgap properties of single crystal materials for infrared detector operation [9,10,11,12]. However, we believe that this approach will add an additional degree of freedom that may be required for certain applications and device architectures.

References

[1] E. Yablanovitch, "Inhibited Spontaneous Emission in Solid-State Physics Electronics", *Physics Review Letters*, **58**, 2059 (1987).

[2] J.D. Joannopoulos, Pierre R. Villeneuve, and Shanhui Fan, "Photonic Crystals: Putting A New Twist On Light", *Nature*, Vol. **386**, 13 March (1997), pp143.

[3] J.H. Holtz and S.A. Asher, "Ploymerized Colloidal Crystal Hydrogel Films as Intelligent Chemical Sensing Materials", *Letters to Nature*, Vol.389, 23 October (1997).

[4] J.M Weissman, H.B. Sunkara, A.S. Tse, and S.A. Asher, "Thermally Switchable Periodicity and Diffraction from Mesoscopic Ordered Materials", *Science*, Vol.274, num.5289, pp959.

[5] Sungwon Kim and Venkatraman Gopalan, "Strain-Tunable Photonic Band Gap Crystals" *Applied Physics Letters* **78,** 3015 (2001).

[6] J.S. Foresi, P.R. Villeneuve, J. Ferrera, E.R. Thoen, G. Steinmeyer, S. Fan, J.D. Joannopoulos, L.C. Kimerling, Henry I. Smith & E.P. Ippen, "Photonic-bandgap microcavities in optical waveguides", *Nature*, Vol. **390**, 13 Nov. (1997), pp143.

[7] W.C. Young, Roak's Formulas for Stress and Strain, sixth edition, McGraw Hill CompanyP714, 1989

[8] Website: http://memsnet.org/material.

[9] P. G. Datskos, S. Rajic, and I. Datskou, "Photo-Induced Stress in Silicon Microcantilevers," *Applied Physics Letters* **73,** 2319 (1998).

[10] P. G. Datskos, S. Rajic, I. Datskou, and C. M. Egert, "Novel Photon Detection Based on Electronically-Induced Stress in Silicon," IR Detectors and Focal Plane Arrays V, SPIE **3978,** 173 (1998).

[11] P. G. Datskos, S. Rajic, C. M. Egert, and I. Datskou, "Detection of Infrared Photons Using the Electronic Stress in Metal-Semiconductor Interfaces," Infrared Technology and Applications XXV, SPIE **3698,** 151 (1999).

[12] P.G. Datskos, S. Rajic, L.R. Senesac, and I. Datskou, " Quantum Well Microcantilever Photon Detectors", *Ultramicroscopy*, **86**, 191 (2001).

Table I. Calculated PBC Suspended Waveguide Resonant Frequencies

Bridge/Waveguide Beam Length (mm)	Diamond (Hz)	Silicon (Hz)	Gallium Arsenide (Hz)	Silicon Nitride (Hz)
0.001	8.49×10^{9}	4.51×10^{9}	3.67×10^{9}	3.58×10^{9}
0.005	3.39×10^{8}	1.80×10^{8}	1.47×10^{8}	1.43×10^{8}
0.010	8.49×10^{7}	4.51×10^{7}	3.67×10^{7}	3.58×10^{7}
0.050	3.39×10^{6}	1.80×10^{6}	1.47×10^{6}	1.43×10^{6}
0.100	8.49×10^{5}	4.51×10^{5}	3.67×10^{5}	3.58×10^{5}
0.500	3.39×10^{4}	1.80×10^{4}	1.47×10^{4}	1.43×10^{4}

All of the beam (waveguide) widths and thicknesses were 0.002 and 0.0005 mm, respectively.

Table II. Dimension change vs device length

Device Length \ Dimension Change	Δ Period	Δ Gap
100 um	7 nm	12 nm
200 um	11 nm	17 nm
400 um	20 nm	27 nm

Table III

Direct-Write Nano-Fab Techniques	SPDT	AFM	FIB	NSOM	EBL
Patterning (X-Y Plane)	100 nm	5 nm	10 nm	20 nm	20 nm
Vertical (Z direction)	20 nm	0.1nm	0.1 nm	0.1 nm	0.1 nm

Figure Captions

Figure 1. Two dimensional photonic crystal surface shown with six hole mirror design along one axis.

Figure 2. Illustration of a one dimensional photonic crystal suspended waveguide with two sets mirrors (holes) separated by a micro-cavity (gap).

Figure 3. Illustration of a tunable photonic bandgap crystal component (node) providing alternate spectral paths depending on the magnitude, frequency, and phase of the applied mechanical stress.

Figure 4. Mechanical modeling results showing the relatively flat stress gradient at particular de-centered locations along a suspended waveguide allowing times of entirely compressive or tensile stress.

Figure 5. Modeling results showing the global and expanded views of the wavelength shift due to mechanical perturbation of the waveguide.

Figure 6. Two views of a suspended waveguide tunable photonic bandgap crystal micro-bridge fabricated with focused ion beam milling and wet sacrificial layer etching on a silicon-on-insulator wafer.

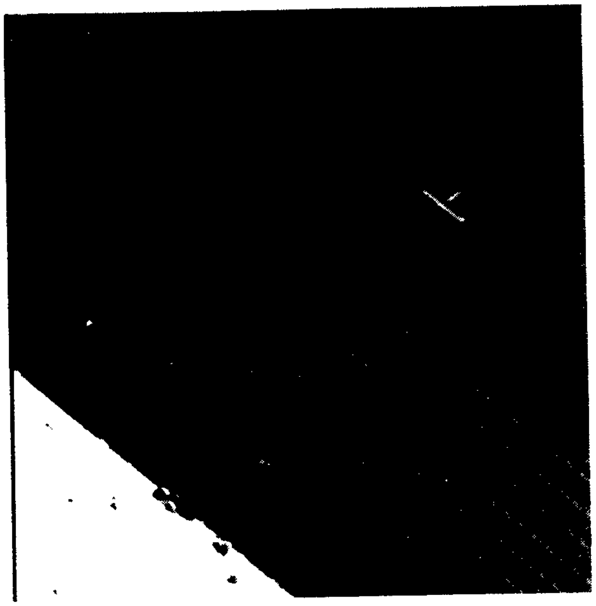

Fig. 1

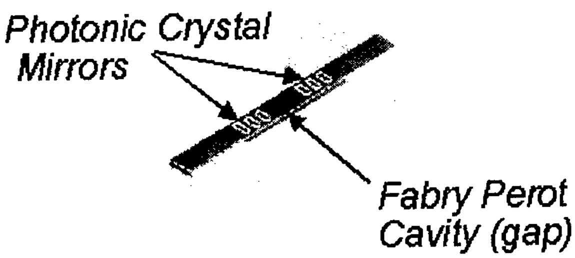

Fig. 2

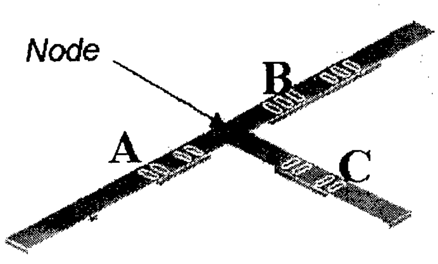

Fig. 3

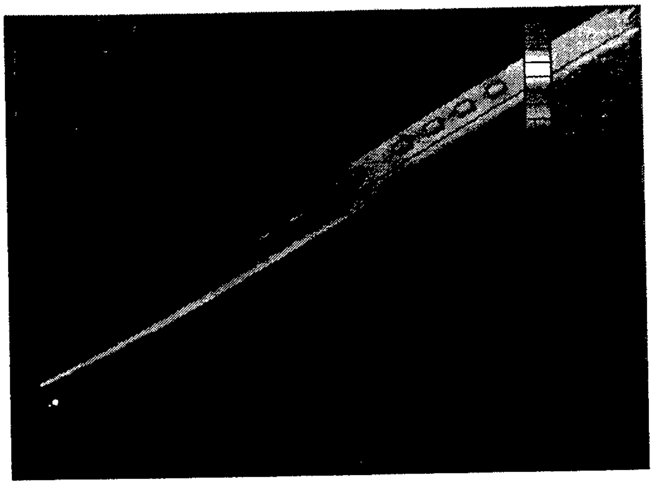

Fig. 4

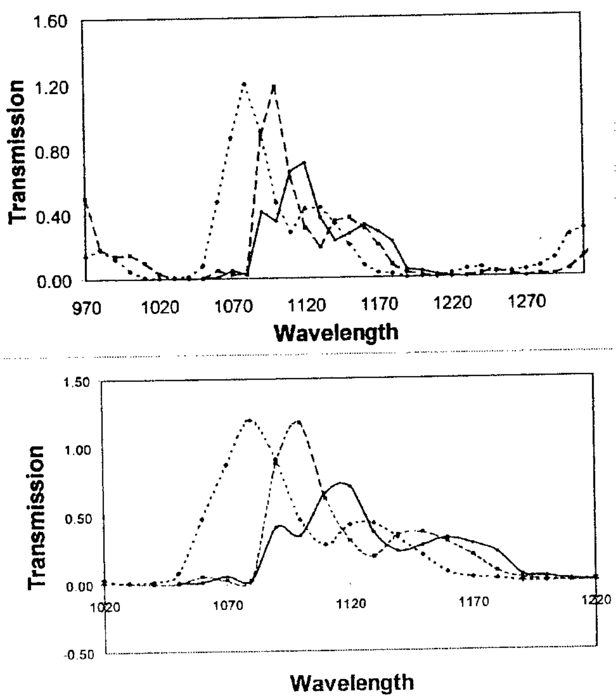

1.60
1.20
0.80
0.40
0.00
Transmission
970
1020
1070
1120
1170
1220
1270
Wavelength
1.50
1.00
0.50
0.00
-0.50
Transmission
1020
1070
1120
1170
1220
Wavelength

Fig. 5